

RSC Advances



This is an *Accepted Manuscript*, which has been through the Royal Society of Chemistry peer review process and has been accepted for publication.

Accepted Manuscripts are published online shortly after acceptance, before technical editing, formatting and proof reading. Using this free service, authors can make their results available to the community, in citable form, before we publish the edited article. This *Accepted Manuscript* will be replaced by the edited, formatted and paginated article as soon as this is available.

You can find more information about *Accepted Manuscripts* in the [Information for Authors](#).

Please note that technical editing may introduce minor changes to the text and/or graphics, which may alter content. The journal's standard [Terms & Conditions](#) and the [Ethical guidelines](#) still apply. In no event shall the Royal Society of Chemistry be held responsible for any errors or omissions in this *Accepted Manuscript* or any consequences arising from the use of any information it contains.

1 **Optimization of bamboo autohydrolysis for the production of**
2 **xylo-oligosaccharides using response surface methodology**

3

4 Xiao Xiao, Chen-Zhou Wang, Jing Bian* and Run-Cang Sun*

5 *Beijing Key Laboratory of Lignocellulosic Chemistry, Beijing Forestry University,*

6 *Beijing 100083, China*

7

8 * Corresponding author. Address: Beijing Key Laboratory of Lignocellulosic Chemistry,

9 Beijing Forestry University, 100083, Beijing, China (Jing Bian and Run-Cang Sun).

10 Tel/Fax: +86 10 62336592 (Jing Bian); +86 10 62336903 (Run-Cang Sun).

11 *E-mail address:* bianjing31@bjfu.edu.cn (Jing Bian); rcsun3@bjfu.edu.cn (Run-Cang

12 Sun);

13

14

15

16

17

18

19

20

21

22

23 **ABSTRACT**

24 Bamboo powder (10.0 g) was subjected to autohydrolysis with a solid to liquid ratio of
25 1:10 under non-isothermal conditions to produce xylo-oligosaccharides (XOS) with a
26 degree of polymerization of 2 to 6. The experiment was performed with two
27 independent variables (reaction temperature 152 - 208 °C and reaction time 1.72 - 58.28
28 min) to optimize the reaction condition by central composite design of response surface
29 methodology. The analysis of variance of the regression model of XOS yield was in
30 good agreement with the experimental results, and the predicted optimal condition for
31 the production of xylo-oligosaccharides was observed at 182 °C for 31 min with the
32 yield of 36.4%. Under the optimal reaction condition for the production of XOS,
33 relatively low concentrations of monosaccharides and byproducts were obtained. The
34 investigation of antioxidant activity revealed that XOS produced from autohydrolysis
35 exhibited a comparable scavenging activity with commercial antioxidant in superoxide
36 and hydroxyl radicals.

37

38

39

40

41

42

43

44

45 **1. Introduction**

46 With the growing emphasis on human health, the production of healthy and
47 economically affordable foods for the world's population has been one of the greatest
48 challenges. Prebiotics are nutrients that have the potential to considerably influence the
49 physiology of human body by promoting the growth of beneficial bifidobacteria in
50 colon, and consequently influence the health.¹ In recent years, more attentions have
51 been paid on the new prebiotics especially xylo-oligosaccharides (XOS). XOS are sugar
52 oligomers made up of 2 to 10 D-xylose units with β -1, 4 bonds, which naturally present
53 in bamboo shoots, fruits, vegetables, milk, and honey.² However, few works are
54 available on the extraction of XOS present in these sources due to their low contents of
55 XOS.

56 Currently, the main process to obtain XOS is to degrade the hemicellulose fraction
57 from carbohydrate-rich lignocellulose by chemical, physical or biological methods. The
58 XOS derived from xylan show various applications in chemical, food, nutraceutical and
59 pharmaceutical industries, which could act as a prebiotics to promote the growth of
60 beneficial bifidobacteria in colon as well as low-calorie sweeteners and antioxidant
61 additives.³ Actually, recent reports show that ingestion of 4 g of XOS per day for 3
62 weeks improves the intestinal microbiota among the elderly who are above 65 years
63 old.^{4,5} Besides, it also has the potential application in agricultural field as fodder
64 additives to enhance the growth of fish, livestock and pets.⁶⁻⁸

65 The main procedure to generate XOS from biomass including enzymatic
66 hydrolysis, dilute acid hydrolysis, and autohydrolysis. The commercial XOS is mainly

67 produced by enzymatic hydrolysis of xylan extracted from biomass by alkaline, which
68 caused the entire deacelation, and exhibits a low solubility in water.³ However, some
69 reports determined that acidic/acetyl XOS (XOS with glucuronic acid/acetyl
70 substitution) shows a high prebiotics benefit as compared to neutral XOS.^{2,9} Due to the
71 formation of too many monosaccharides as compared with XOS, and the large amount
72 of toxic byproducts such as furfural and 5-hydroxymethylfurfural (HMF), diluted acid
73 hydrolysis has limited application.⁵ Autohydrolysis, an effective procedure to produce
74 XOS, is well known as an environmentally friendly and economical technology. In
75 autohydrolysis, hydronium ions derived from the autoionization of water act as a
76 catalyst cause the depolymerization of hemicelluloses to XOS, xylose and other sugar
77 degradation products. The partial cleavage of acetyl groups to acetic acids during the
78 autohydrolysis process results in the increase of hydronium ions concentration in the
79 reaction media, which also promote the hydrolysis efficiency. As an effective method to
80 produce oligosaccharides, autohydrolysis has the advantages of no chemical regents and
81 high selectivity separation. There are a lot of reports about XOS produced by
82 autohydrolysis from corncob wheat straw, rye straw, etc.¹⁰⁻¹² The biological activity of
83 XOS is mainly influenced by the degree of polymerization and substitutions.^{13,14} Some
84 recent studies show that the XOS with low DP is of particular interest for prebiotic
85 applications. XOS with DP from 2 to 6 are non-digestible oligosaccharides (NDOs),
86 which show high value in food additives industries.¹⁵ However, the XOS produced in
87 the above studies exhibited a wide range of degree of polymerization of 2 to 20.¹⁰⁻¹²
88 Previous study investigated the production of XOS by autohydrolysis, which contains a

89 large portion of high DP XOS (>6).³ Bamboo powder was employed as the raw material
90 for autohydrolysis in the present work, since it has advantages of easy propagation,
91 rapid growth and high productivity. Furthermore, some reports show that XOS derived
92 from bamboo have a cytotoxic effect on human leukemia cells.¹⁶ In this study, the
93 autohydrolysis process was optimized to find the best reaction condition for the
94 production of XOS (DP 2-6) by using response surface methodology (RSM), and the
95 influence of reaction temperature and time on the yield of XOS was investigated.³ The
96 monosaccharides, byproducts and the antioxidant activity of XOS were also detected.³

97

98 **2. Materials and methods**

99 **2.1. Raw materials**

100 Bamboo culms were collected in July, 2014 from Yunnan province, China. The raw
101 material was dried in an oven at 60 °C for 24 h and then ground in a mill to obtain a
102 fraction of 40 to 80 mesh. After that, the obtained bamboo powder was dewaxed with
103 toluene-ethanol (2:1 v/v) in a Soxhlet extractor for 6 h and destarched with water at 80
104 °C for 6 h. The extractive-free sample was dried in an oven at 60 °C for 12 h and stored
105 for further use.³ The standards of xylobiose, xylotriose, xylotetraose, xylopentaose and
106 xylohexaose were purchased from Megazyme (Ireland), and other chemicals were
107 provided by Sigma-Aldrich.

108

109 **2.2. Autohydrolysis process**

110 Bamboo samples (10.0 g, oven-dried basis) and deionized water were mixed in a 1 L

111 stainless steel autoclave with mechanical stirring (Parr, USA) at a solid to liquor ratio of
112 1:10 g/g. The autoclave was heated by an external electrical furnace with the agitation
113 of 150 rpm, and the reaction temperature was measured with a type-J thermocouple for
114 different reaction times. A Proportional-Integral-Derivative (PID) controller was
115 employed to dominate the temperature, and cooling of the mixture was accomplished by
116 using circulating cold water.

117

118 **2.3. Analysis of autohydrolysis liquors**

119 The liquors obtained by the autohydrolysis were filtered and stored to determine
120 monosaccharides, XOS and sugar degradation products. A high-performance
121 anion-exchange chromatography (HPAEC, Dionex ICS-3000, USA) system equipped
122 with a Carbopac PA-20 column (4×250 mm, Dionex, USA), and a Carbopac PA-100
123 column (4×250 mm, Dionex, USA) was employed to quantify the monosaccharides and
124 oligosaccharides in the liquor. The eluent of 100 mM NaAc in a 150 mM NaOH at a
125 flow rate of 0.4 mL/min and a column temperature of 30 °C was used to separate the
126 XOS. The degradation products were quantified and analyzed by an high-performance
127 liquid chromatography (HPLC, Agilent 1200 series, Agilent Technologies, USA)
128 equipped with a refractive index detector using a HPX-87H ion exclusion column
129 (7.8×300 mm, Bio-Rad Laboratories, USA). The mobile phase was 0.005M sulfuric
130 acid at flow rate of 0.6 mL/min with the column temperature of 50 °C. More details of
131 the analysis method were described in the previous literatures.^{3, 17}

132

133 2.4. Experimental design

134 The autohydrolysis variables were studied to determine the optimal conditions for the
135 maximum xylo-oligosaccharides yield. The influences of temperature and reaction time
136 were determined through a response surface methodology, and central composite design
137 (CCD) with a total of 11 experiments was employed to determine the best combination
138 of parameters for the autohydrolysis process. Four axial points, four fractional points
139 and three center points were carried out with the alpha factor of 1.414 for rotatable
140 design. The yield of XOS was determined as the response variable Y. The variables
141 were coded according to the equation:

$$142 \quad x_i = (X_i - X_{i,0}) / \Delta X_i \quad (i=1, 2) \quad (1)$$

143 where x_i is the coded value of the variable X_i , $X_{i,0}$ is the real value of X_i at the center
144 point, and ΔX_i is the step change.

145 The relationship of the variables and response was calculated by the quadratic
146 regression equation:^{18, 19}

$$147 \quad Y = \beta_0 + \sum_{i=1}^k \beta_i X_i + \sum_{i=1}^k \beta_{ii} X_i^2 + \sum_{1 \leq i < j}^k \beta_{ij} X_i X_j \quad (2)$$

148 where k is the number of variables, X_i and X_j are independent variables, which influence
149 the response variable Y , β_0 is the constant term, β_i represents the coefficients of the
150 linear parameters, β_{ii} is the quadratic coefficient and β_{ij} estimates the interaction
151 parameters.

152 The conditions of each run are shown in Table 1. The results were summarized and
153 statistically analyzed by using Design-Expert software (version 8.0.6, StatEase Inc.,
154 USA). Analysis of variance (ANOVA) was employed to estimate the regression model.

155

156 **2.5. Antioxidant activities**

157 The phenazine-methosulfate (PMS)-NADH method was employed for the generation of
158 O_2^- to investigate the superoxide radical scavenging assay.²⁰ The mixture containing
159 varying concentrations of XOS samples (1 mL, 0.05-2 mg/mL), PMS (1 mL, 60 μ M),
160 NADH (1 mL, 676 μ M), and NBT (1mL, 144 μ M) in phosphate buffer (0.1 M, pH 7.4)
161 was incubated at room temperature for 5 min. The mixture was shaken for 1 h, and then
162 absorption was measured at 560 nm. The capability of scavenging to superoxide radical
163 was calculated using the following formula:

$$164 \text{ Superoxide radical scavenging effect (\%)} = (1 - A_1/A_0) \times 100\% \quad (3)$$

165 where A_1 is the absorbance of the sample mixed with reaction solution, and A_0 is the
166 absorbance of control. Superoxide radical scavenging assay was plotted as a function of
167 XOS concentration. From this graph, the XOS concentration needed to achieve
168 superoxide radical scavenging activity of 50% was defined as IC_{50} . Radical scavenging
169 index (RSI) was defined as the inverse of IC_{50} . The analysis was performed in triplicate.

170 The Fenton's system ($Fe^{2+} + H_2O_2 \rightarrow Fe^{3+} + OH^- + OH\cdot$) was employed to investigate
171 the hydroxyl radical scavenging assay of the XOS samples. The method was conducted
172 according to the previous literature reported by Smirnoff and Cumbe, and hydroxyl
173 radical was produced by the solution containing 2 mM EDTA- Fe^{2+} (0.5 mL), 3% H_2O_2
174 (1 mL), 360 μ g/mL crocus in 4.5 mL sodium phosphate buffer (150 mM, pH7.4).^{21, 22}
175 Subsequently, the XOS samples with different concentrations were added, and the
176 mixtures were incubated at room temperature for 30 min. The capabilities of scavenging

177 hydroxyl radical of the mixtures were measured at 520 nm using a UV 2300
178 spectrometer (Thermal Scientific, USA), and calculated using the following formula:
179 Hydroxyl radical scavenging effect (%) = $(1 - A_I/A_0) \times 100\%$ (4)
180 where A_I is the absorbance of the samples, and A_0 is the absorbance of control. The
181 concentration required to quench 50% of the initial hydroxyl radical was defined as IC₅₀,
182 and the analysis was performed in triplicate.

183 The free radical-scavenging activity was measured by the effect of scavenging
184 2,2-diphenyl-1-picrylhydrazyl radicals (DPPH) according to Li et al.²³ 0.2 mM DPPH
185 solution in 50% methanol was prepared before UV measurements, and then different
186 concentrations of XOS samples (1 mL) were thoroughly mixed with 2 mL of freshly
187 prepared DPPH and 2 mL of methanol. The mixture was shaken vigorously and kept in
188 the dark at room temperature for 30 min. The capabilities of the samples to scavenge the
189 DPPH radicals were calculated using the following equation:

$$190 \text{ DPPH radical scavenging effect (\%)} = (1 - A_I/A_0) \times 100\% \quad (5)$$

191 where A_0 is the absorbance of control, and A_I is the absorbance of the sample. The
192 concentration of the samples needed to achieve DPPH radical-scavenging activity of
193 50% was defined as IC₅₀, and the analysis was performed in triplicate.

194

195 **3. Results and discussion**

196 **3.1. Composition of the raw materials**

197 The composition of the extractive-free bamboo powder was determined by the NREL
198 laboratory analytical procedure.²⁴⁻²⁶ As described in the precious literature, the

199 composition of destarched sample was ash 2.8%, moisture 9.3%, and lignin 25.9%
200 (Klason lignin 24.1% and acid-soluble lignin 1.8%). Cellulose (40.4%) was the most
201 significant portion of biomass, and hemicelluloses (21.6%) were measured as xylan
202 substituted with arabinose (0.8%), galactose (0.2%), mannose (0.1%), glucuronic acid
203 (0.1%) and acetyl groups (2.2%). The ratio of acetyl group to xylose was 0.27 mol/mol.³

204

205 **3.2. Central Composite Design Model Fitting**

206 Response surface methodology is an effective statistical method using quantitative data
207 from an appropriate experiment design to investigate and to simultaneously solve
208 multivariate equations, which has the advantages of reducing set of experiments to
209 determine the interactions of a mathematical model and the optimum conditions.²⁷ Thus,
210 the reaction temperature and time were examined as factors to investigate the
211 correlation between the autohydrolysis variables to the XOS yield by using CCD. The
212 complete experiment variables design matrix together with the values of experimental
213 responses is presented in Table 1, and the ANOVA was carried out to select a suitable
214 model, to detect the significances of the model equation, and to investigate the model
215 terms. The following equation represents the description of XOS (2-6) yields from the
216 experimental responses:

$$217 \quad Y=35.98+2.88X_i+1.63X_j-6.65X_iX_j-13.89X_i^2-14.26X_j^2$$

218 where X_i and X_j are represent reaction temperature and time, respectively.

219 In order to acquire a best fit model, ANOVA was employed to identify the adequacy
220 of the models. The ANOVA data are summarized in Tables 2 and 3, in which the

221 coefficient of determination R^2 was defined to explain variation to the total variation
222 and to demonstrate the agreement between the observed and predicted results. It was
223 suggested that R^2 value should be at least 0.80 for a good fit of a model. A high R^2
224 represents that predicted values for XOS yield are more accurate and closer to the actual
225 values. The R^2 (0.9823) in the present work (Table 2) indicated that 98.23% total
226 variation in XOS yield was attributed to the experimental variables. This illustrated that
227 a high correlation between the experimental values and theoretical predicts could be
228 observed by the model and expressed good enough fit (Fig. 1). Additionally, the Pred.
229 R^2 of 0.8741 was in reasonable agreement with the Adj. R^2 of 0.9646, exhibited a good
230 adjustment between the experiment and predicted values. As shown in Table 2, standard
231 deviation and coefficient of variation percent (CV %) in the present study were
232 reasonably low and acceptable, indicated a high reliability of the experiment.

233 The probability value (P -value) was employed to check the significance of the
234 coefficient, indicating the interaction between each independent variable.¹⁸ P -values
235 <0.05 for the regression model are statistically significant. In the present work the
236 P -value of the model (0.0002) was significant enough with significance in lack of fit of
237 0.0016. The analysis also showed that P -values of X_i , X_j , X_iX_j , X_i^2 and X_j^2 were 0.0289,
238 0.1455, 0.0043, <0.0001 and <0.0001 , respectively, demonstrating that the variables X_i ,
239 and quadratic variables X_iX_j , X_i^2 and X_j^2 affect XOS yield outstandingly. This illustrated
240 that the reaction temperature and time significantly affected the production of XOS, and
241 as compared with reaction time, the reaction temperature has a smaller P -value. The
242 variables with smaller P -value showed a higher significance of the corresponding

243 coefficient, indicated that the effect of reaction temperature (0.0289) on the production
244 of XOS was greater than that of reaction time (0.1455). Additionally, *F*-value is another
245 factor implies that the response surface model is significant.²⁸ In the current study,
246 *F*-value of 55.42 (Table 3) indicated that there was only a 0.02% chance that a “Model
247 *F*-value” this large could occur due to noise.

248

249 **3.3. Optimization of the production of xylo-oligosaccharides**

250 Response surface plots were built up by plotting the response (XOS production) against
251 two independent variables to identify the optimal conditions of each variable for
252 maximum XOS yield. Two-dimensional contour plots and three-dimensional response
253 surface plots in the present work were generated by Design-Expert as shown in Fig. 2.
254 In Figs. 2a and b, a quadratic effect of both reaction temperature and time was observed,
255 although temperature had a greater influence on the response. The benefit of reaction
256 temperature on XOS yield was observed in the range of 152-180 °C, and a further
257 increase in reaction temperature resulted in a rapid decline. On the other hand, similar
258 phenomenon could be found in reaction time, which positively affected the XOS yield
259 from 0 to 30 min, but led to the decrease after 30 min reaction. The decrease trend of the
260 yield was mainly due to the excessive degradation of xylan with both the raise of the
261 temperature and prolongation of time. The longer reaction time and/or higher reaction
262 temperature would generate more xylose and sugar degradation products, leading to the
263 decline of the XOS yield. The result illustrated that both variables significantly affected
264 the production of XOS, and the optimal reaction condition was obtained. In Fig. 2b, the

265 red zone represents the optimal reaction condition for the production of XOS, and the
266 predicted optimal point was observed (182 °C and 31 min). This indicated that the
267 production of XOS achieved the highest yield (36.1 %) at 182 °C for 31 min reaction,
268 which was a relatively high yield as compared with the result of enzymatic hydrolysis
269 (31.8%) and diluted acid (13%) hydrolysis.^{18, 29}

270 An additional experiment run was conducted under the predicted condition to verify
271 the present suggested model. Experimentally, the XOS yield of the autohydrolysis
272 reaction at 182 °C after 31 min was 36.4%, which showed no remarkable difference to
273 the predicted value, indicated that the model can mathematically represent XOS
274 production by autohydrolysis with the coefficient of 0.98. Furthermore, a relatively low
275 yield of monosaccharides and sugar degradation products were observed under the
276 optimal reaction condition, which was benefit for the further purification and utilization
277 of XOS (Table 1 and Fig. 3, the details will be discussed in the following parts).

278

279 **3.4. Formation of monosaccharides and degradation products during** 280 **autohydrolysis process**

281 The liquors after autohydrolysis reaction contained not only XOS, but also a number of
282 monosaccharides and sugar degradation products (acetic acid, formic acid, furfural and
283 5-hydroxymethylfurfural, etc.). In the present study, the monosaccharides were detected
284 by HPAEC and the sugar degradation products were determined by HPLC. As the data
285 presented in Table 1 and Fig. 3, a lot of monosaccharides and sugar degradation
286 products were generated during the autohydrolysis process apart from XOS, especially

287 at a high temperature with a long reaction time. The concentration of monosaccharides
288 increased with the raise of reaction temperature and prolongation of reaction time, and
289 the highest values were achieved at 180 °C for 58.28 min (arabinose 0.43 g/L, galactose
290 0.25 g/L, glucose 2.58 g/L and xylose 6.34 g/L). However, a further increase in reaction
291 temperature and time caused a rapid decline of the concentration of monosaccharides,
292 which could be interpreted by the fact that a part of pentose and hexose were degraded
293 into furfural and HMF under the intensive reaction conditions. Moreover, the result also
294 revealed that the formation rate of monosaccharides was much lower than that of the
295 degradation rate, which led to the rapid decline of the concentration, could be certified
296 by the data of sugar degradation products. On the other hand, the concentration
297 variation of monosaccharides indicated that α -1, 2 and α -1, 3 bond cleaved in the early
298 stage due to the relatively high concentration of arabinose at a low reaction temperature.
299 In Fig. 3, the concentration of arabinose at a low reaction temperature was higher as
300 compared with others, demonstrated that arabinose was easier cleaved from xylan
301 backbone. The variation trends also revealed that arabinose was easier to be degraded
302 into furfural since the concentration decreased at 180 °C after 30 min (0.56 to 0.42 g/L
303 from 30 to 58.28 min).

304 Besides oligosaccharides and monosaccharides, some byproducts would be
305 performed during autohydrolysis process, especially under an intensive reaction
306 condition. Table 1 presents the main byproducts formatted during the reaction period,
307 which were furfural, HMF, acetic acid and formic acid. Furfural and HMF were the
308 degradation products of pentose and hexose, respectively, whose yield were remarkably

309 affected by the reaction temperature and time. As seen in Table 1, the maximum
310 concentrations of furfural and HMF in the present work were observed when the
311 reaction was conducted at an axial point (208.28 °C, 30 min; furfural 4.12 g/L, HMF
312 1.80g/L). The result revealed that the production of furfural and HMF exhibited a
313 positive correlation with the reaction temperature. On the other hand, as the data shown
314 in Table 1, the concentrations of furfural and HMF increased (the concentration of
315 furfural and HMF raised from 0 to 1.63 g/L and 0 to 0.36 g/l, respectively) with the
316 prolongation of reaction time (from 1.72 to 58.28 min) when the temperature was 180
317 °C, which indicated that a longer reaction time led to a higher concentration of furfural
318 and HMF. These results demonstrated that large amounts of the sugar degradation
319 product would be generated under the intensive reaction conditions. Since furfural and
320 HMF have negative effects on the further utilization of XOS, the formation of sugar
321 degradation products should be avoided during the XOS production process, which is
322 beneficial to the prospective purification and utilization. The concentrations of furfural
323 and HMF at the optimal reaction point (182 °C and 31 min) in the present work were
324 0.59 and 0.12 g/L, respectively, which were comparatively low to the XOS yield of
325 36.4% (equivalent to 7.85 g/L). In comparison to others, the result of furfural and HMF
326 in present study was lower than previous literatures of autohydrolysis and diluted acid
327 hydrolysis, which was positive for the further utilization of XOS.^{30,31}

328 Acetic acid is one of the main byproducts generated during autohydrolysis process,
329 which is produced by the release of acetyl groups attached on the xylan chain.
330 Additionally, it could be obtained by the degradation of furfural and HMF. The ester

331 linkage was cleaved when the autohydrolysis was conducted at a high temperature, and
332 led to the release of acetyl groups and the formation of acetic acid in the reaction media.
333 The acetic acid generated during the autohydrolysis process would be a diluted acid
334 catalyst and caused the decline of pH, resulted in the promotion of the reaction. The
335 concentration of acetic acid produced in the present study is shown in Table 1, where
336 the concentration was increased with the raise of reaction temperature and/or
337 prolongation of reaction time. Similar situation could be found in pH, which declined
338 with the raise of reaction temperature and/or prolongation of reaction time, indicating a
339 negative linear correlation with acetic acid concentration. Furthermore, the maximum
340 acetic acid concentration of 1.68 g/L was obtained at an axial point (208.28 °C, 30 min),
341 which also have the lowest pH (2.66) in the present work. However, under the optimal
342 reaction condition for XOS production (182 °C, 31 min), the detected acetic acid
343 concentration was only 0.61 g/L, equivalent to 18.9% of the initial acetyl groups. It
344 means that large amounts of acetyl groups were still attached on the chain of XOS in the
345 liquor and xylan in the residue. The previous findings in biology activity of XOS
346 revealed that the *in vitro* fermentation of acetylated XOS was much slower than that of
347 neutral XOS, which produced more organic acids, resulted in the promotion in the
348 prebiotic effect.^{14, 32} The current result of acetic acid indicated that a lot of XOS
349 obtained in the present work was substituted with acetyl groups, which was positive for
350 the prospective utilization. Formic acid is another weak acid which could be presented,
351 and it is formed by the degradation of furfural and HMF during autohydrolysis
352 process.³³ Thus, formic acid could only be observed at a high reaction temperature, and

353 it also played a role in diluted acid catalyst in the reaction. Similarly, the concentration
354 of formic acid was increased with the raise of reaction temperature and prolonging of
355 time, and the maximum formic acid concentration of 0.71 g/L was obtained at 200 °C
356 for 50 min. In addition, only 0.17 g/L formic acid was observed under the predicted
357 optimal reaction condition (182 °C, 31 min) in the present study, which was fairly low
358 as compared with the XOS yield.

359 In autohydrolysis process, hemicelluloses were degraded first at a low temperature
360 followed by lignin decomposed at intermediate temperature. Previous research about the
361 wheat bran showed that the lignin started to degrade at 170 °C and achieved to the
362 highest degradation at 220 °C, in which 30% of the initial ferulic acid was released into
363 the reaction media.³⁴ In the present study, the degradation was occurred, which 9.7% of
364 the initial lignin was released under the optimal reaction condition (182 °C, 31 min).
365 The degradation compounds might be the ferulic acid, p-coumaric acid, and lignin
366 degradation products, which would be exactly investigated in our following studies.³⁵

367

368 **3.5. Antioxidant activities of XOS**

369 The antioxidant activity of XOS samples was investigated in comparison with
370 commercial antioxidants by three different methods. BHA and BHT are the two
371 commercial antioxidants control group, and the curves of the inhibitory effects of these
372 specimens are shown in Fig. 4. The XOS sample was generated under the optimal
373 reaction conditions (182 °C and 31 min).

374 Superoxide radical is the one of the oxygen radicals, which leads to H₂O₂ formation

375 by indirectly initiate lipid peroxidation, creating precursors of hydroxyl radicals.³⁶ The
376 superoxide radical scavenging ability is obviously significant for the antioxidant
377 research, and Fig. 4a shows the superoxide radical scavenging activity of XOS samples
378 in the present work, and the radical-scavenging index (RSI) values of BHA, BHT and
379 XOS were 0.21, 0.79 and 0.95, respectively. Obviously, the result indicated that the
380 superoxide radical scavenging activity of all samples showed a concentration-dependent,
381 and BHA exhibited highest scavenging ability. The scavenging activity of XOS was
382 close to that of BHT, which demonstrated that the XOS obtained by autohydrolysis
383 exhibited an acceptable superoxide radical scavenging activity.

384 Hydroxyl radical is the most active oxygen radical, which induces severe damage to
385 the adjacent molecule.³⁷ The superoxide radical scavenging activity of XOS samples in
386 the present work is shown Fig. 4b. It could be observed that the superoxide radical
387 scavenging activity of the samples raised with the increase of the concentration.
388 Moreover, the RSI value of XOS was 0.65, as compared to 0.17 for BHA and 0.57 for
389 BHT, respectively. This suggested that the XOS presented a comparable scavenging
390 activity with BHT, whereas the scavenging activity of BHA was much better than that
391 of BHT and XOS.

392 The investigation of scavenging activity of DPPH radical is a common procedure
393 for the evaluation of the free radical scavenging ability of natural products. The
394 scavenging ability of XOS obtained by autohydrolysis at optimal predicted reaction
395 condition is shown in Fig. 4c. The result suggested that all samples (BHA, BHT and
396 XOS) exhibited concentration-dependent antioxidant activity, and the RSI values of

397 BHA, BHT and XOS were 0.07, 0.34 and 0.84, respectively. The scavenging activity of
398 BHA increased rapidly with the growing concentration, while that of XOS exhibited a
399 relatively flat growth. The percent of inhibition of XOS gradually increased and reached
400 86.4% at the concentration of 2 mg/mL. Meanwhile, the DPPH radical scavenging
401 activity of XOS obtained in the present work was higher than that of maize XOS and
402 sugarcane bagasse XOS produced by enzymatic hydrolysis as reported in previous
403 literatures, which may be due to the presence of phenolic compounds degraded from
404 lignin during autohydrolysis process.^{38, 39} The phenolic compounds in the obtained
405 liquor by autohydrolysis might enhance the antioxidant activity of XOS. According to
406 the previous literature, the antioxidant activity would decline after the purification of
407 XOS, since the degraded products had a positive effect on antioxidant activity and
408 would be removed.³⁹ Besides, type of phenolic acids, the effects of degree of
409 polymerization, linkage type, substituted groups and position, ester linked phenolic
410 acids, and the presence of sugars with uronic/acetyl groups cannot be underestimated
411 since they played a very important role in the antioxidant activity of the XOS produced
412 by autohydrolysis.³⁹

413

414 **4. Conclusion**

415 Bamboo powder was autohydrolyzed in a stainless steel autoclave to generate
416 xylo-oligosaccharides with low a degree of polymerizations (DP 2-6). The reaction
417 temperature and time significantly affected the production of XOS, and the optimal
418 reaction condition was observed by using response surface methodology. The analysis

419 indicated that autohydrolysis conducted at 182 °C for 31 min achieved the maximum
420 XOS yield of 36.4% with a relatively low concentration of monosaccharides and
421 byproducts. The investigation of antioxidant activity revealed that XOS by
422 autohydrolysis exhibited an acceptable scavenging activity in superoxide radical and
423 hydroxyl radical as compared with the commercial antioxidant BHT.

424

425 **Acknowledgements**

426 The authors are grateful for the kind support from the Beijing Natural Science
427 Foundation (6154031), the National Natural Science Foundation of China (31400508,
428 31430092), Open Foundation of State Key Laboratory of Pulp and Papermaking
429 Engineering, South China University of Technology (No 201402).

430

431

432

433

434

435

436

437

438

439

440

441 **References**

- 442 1 G. R. Gibson and M. B. Roberfroid, *The Journal of Nutrition*, 1995, 125, 1401-1412.
- 443 2 A. A. Achary and S. G. Prapulla, *Comprehensive Reviews in Food Science and*
444 *Food Safety*, 2011, 10, 2-16.
- 445 3 X. Xiao, J. Bian, X. P. Peng, H. Xu, B. Xiao and R. C. Sun, *Bioresour Technol*, 2013,
446 138, 63-70.
- 447 4 Y. C. Chung, C. K. Hsu, C. Y. Ko and Y. C. Chan, *Nutr Res*, 2007, 27, 756-761.
- 448 5 D. O. Otieno and B. K. Ahring, *Bioresour Technol*, 2012, 112, 285-292.
- 449 6 B. Xu, Y. Wang, J. Li and Q. Lin, *Fish Physiol Biochem*, 2009, 35, 351-357.
- 450 7 P. Gullon, G. Pereiro, J. L. Alonso and J. C. Parajo, *Bioresour Technol*, 2009, 100,
451 5840-5845.
- 452 8 P. Moura, S. Marques, L. Alves, J. P. B. Freire, L. F. Cunha and M. P. Esteves,
453 *Livestock Science*, 2007, 108, 244-248.
- 454 9 P. Christakopoulos, P. Katapodis, E. Kalogeris, D. Kekos, B. J. Macris, H. Stamatis
455 and H. Skaltsa, *Int J Biol Macromol*, 2003, 31, 171-175.
- 456 10 G. Garrote, J. M. Cruz, H. Dominguez and J. C. Parajo, *J Chem Technol Biotechnol*,
457 2003, 78, 392-398.
- 458 11 D. Nabarlitz, A. Ebringerová and D. Montané, *Carbohydr Polym*, 2007, 69, 20-28.
- 459 12 B. Gullon, R. Yanez, J. L. Alonso and J. C. Parajo, *Bioresour Technol*, 2010, 101,
460 6676-6684.
- 461 13 S. A. Hughes, P. R. Shewry, L. Li, G. R. Gibson, M. L. Sanz and R. A. Rastall, *J*
462 *Agric Food Chem*, 2007, 55, 4589-4595.

- 463 14 K. M. J. Van Laere, R. Hartemink, M. Bosveld, H. A. Schols and A. G. J. Voragen,
464 J Agric Food Chem, 2000, 48, 1644-1652.
- 465 15 S. I. Mussatto and I. M. Mancilha, Carbohydr Polym, 2007, 68, 587-597.
- 466 16 H. Ando, H. Ohba, T. Sakaki, K. Takamine, Y. Kamino, S. Moriwaki, R. Bakalova,
467 Y. Uemura and Y. Hatate, Toxicol In Vitro, 2004, 18, 765-771.
- 468 17 F. Peng, J. L. Ren, F. Xu, J. Bian, P. Peng and R. C. Sun, J Agric Food Chem, 2009,
469 57, 6305-6317.
- 470 18 J. Bian, P. Peng, F. Peng, X. Xiao, F. Xu and R. C. Sun, Food Chem, 2014, 156,
471 7-13.
- 472 19 T. Yoshida, S. Tsubaki, Y. Teramoto and J. Azuma, Bioresour Technol, 2010, 101,
473 7820-7826.
- 474 20 J. Robak and R. J. Gryglewski, Biochem Pharmacol, 1988, 37, 837-841.
- 475 21 N. Smirnov and Q. J. Cumbes, Phytochemistry, 1989, 28, 1057-1060.
- 476 22 J. Wang, F. Wang, Q. B. Zhang, Z. S. Zhang, X. L. Shi and P. C. Li, Int J Biol
477 Macromol, 2009, 44, 379-384.
- 478 23 M.-F. Li, S.-N. Sun, F. Xu and R.-C. Sun, Food Chem, 2012, 134, 1392-1398.
- 479 24 A. Sluiter, B. Hames, R. Ruiz, C. Scarlata, J. Sluiter and D. Templeton, Technical
480 Report, 2005, NREL/TP-510-42622.
- 481 25 A. Sluiter, B. Hames, D. Hyman, C. Payne, R. Ruiz, C. Scarlata, J. Sluiter, D.
482 Templeton and J. Wolfe, Technical Report, 2008, NREL/TP-510-42621.
- 483 26 A. Sluiter, B. Hames, R. Ruiz, C. Scarlata, J. Sluiter, D. Templeton and D. Crocker,
484 Technical Report, 2008, NREL/TP-510-42618.

- 485 27 J. Chen, D. Liu, B. Shi, H. Wang, Y. Cheng and W. Zhang, *Carbohydr Polym*, 2013,
486 93, 81-88.
- 487 28 B. Satari Baboukani, M. Vossoughi and I. Alemzadeh, *Biosyst Eng*, 2012, 111,
488 166-174.
- 489 29 O. Akpinar, K. Erdogan and S. Bostanci, *Carbohydr Res*, 2009, 344, 660-666.
- 490 30 G. Garrote, H. Domínguez and J. C. Parajó, *Journal of Chemical Technology &*
491 *Biotechnology*, 1999, 74, 1101-1109.
- 492 31 D. Nabarlatz, X. Farriol and D. Montane, *Ind Eng Chem Res*, 2005, 7746-7755.
- 493 32 H. Pastell, P. Westermann, A. S. Meyer, P. Tuomainen and M. Tenkanen, *J Agric*
494 *Food Chem*, 2009, 57, 8598-8606.
- 495 33 F. Carvalheiro, M. P. Esteves, J. C. Parajo, H. Pereira and F. M. Girio, *Bioresour*
496 *Technol*, 2004, 91, 93-100.
- 497 34 D. J. Rose and G. E. Inglett, *J Agric Food Chem*, 2010, 58, 6427-6432.
- 498 35 D. J. Yelle, P. Kaparaju, C. G. Hunt, K. Hirth, H. Kim, J. Ralph and C. Felby,
499 *Bioenerg Res*, 2012, 6, 211-221.
- 500 36 Y. J. Sun, B. Y. Yang, Y. M. Wu, Y. Liu, X. Gu, H. Zhang, C. J. Wang, H. Z. Cao, L.
501 J. Huang and Z. F. Wang, *Food Chem*, 2015, 178, 311-318.
- 502 37 O. Erel, *Clin Biochem*, 2004, 37, 112-119.
- 503 38 J. Bian, F. Peng, X.-P. Peng, P. Peng, F. Xu and R.-C. Sun, *Bioresour Technol*,
504 2013, 127, 236-241.
- 505 39 B. R. Veenashri and G. Muralikrishna, *Food Chem*, 2011, 126, 1475-1481.
- 506

Figure captions

Fig. 1. The correlation between predicted and actual values.

Fig. 2. Response surface (a) and contour plot (b) of XOS yield.

Fig. 3. Concentration of monosaccharides generated during autohydrolysis.

Fig. 4. Scavenging activity of superoxide radical (a), hydroxyl radical (b) and DPPH free-radical (c) of XOS.

Table 1 Experimental design (independent variables), pH, response and byproducts of the CCD.

Run	Coded variables		Real variables		pH	Response	Sugar degradation products (g/L)			
	X_i	X_j	Temp. (°C)	Time (min)		XOS yield (%)	Acetic acid	Formic acid	Furfural	HMF
1	-1	1	160	50	3.11	14.0	0.23	n.d. ^a	0.07	n.d.
2	0	0	180	30	3.02	36.0	0.57	0.16	0.53	0.07
3	0	1.414	180	58.28	2.77	10.1	0.81	0.38	1.63	0.36
4	-1	-1	160	10	3.71	0.1	0.11	n.d.	n.d.	n.d.
5	1.414	0	208.28	30	2.66	11.5	1.68	0.66	4.12	1.80
6	1	1	200	50	2.68	5.4	1.66	0.71	3.80	1.55
7	0	-1.414	180	1.72	3.65	1.7	0.14	n.d.	n.d.	n.d.
8	0	0	180	30	2.92	35.8	0.58	0.17	0.53	0.07
9	0	0	180	30	2.98	36.1	0.61	0.16	0.52	0.09
10	-1.414	0	151.72	30	3.50	1.8	0.09	n.d.	n.d.	n.d.
11	1	-1	200	10	2.86	18.1	1.07	0.23	1.02	0.23

^a n.d., not detected

Table 2 Statistical parameters of ANOVA of the XOS predicted model.

Statistical Parameter	Value	Statistical Parameter	Value
Std. Dev.	2.6819	R ²	0.9823
Mean	15.507	Adj R ²	0.9646
C.V. %	17.2953	Pred R ²	0.8741
PRESS	255.5708	Adeq Precision	19.8443

Table 3 Analysis of variance of the model for XOS yields.

Source	Sum of Squares	Degree of Freedom	Mean Square	F-Value	<i>p</i> -value Prob > F
Model	1993.33	5	398.67	55.42	0.0002
X_i	66.31	1	66.31	9.22	0.0289
X_j	21.35	1	21.35	2.97	0.1455
$X_i X_j$	176.91	1	176.91	24.59	0.0043
X_i^2	1089.33	1	1089.33	151.44	< 0.0001
X_j^2	1147.58	1	1147.58	159.54	< 0.0001
Residual	35.97	5	7.19		
Lack of Fit	35.93	3	11.98	640.13	0.0016
Pure Error	0.037	2	0.019		
Corrected Total	2029.29	10			

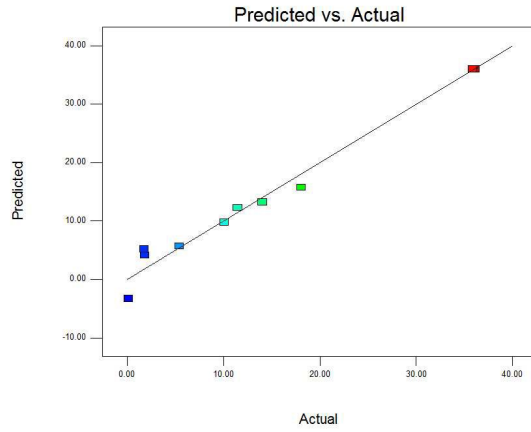


Fig. 1.

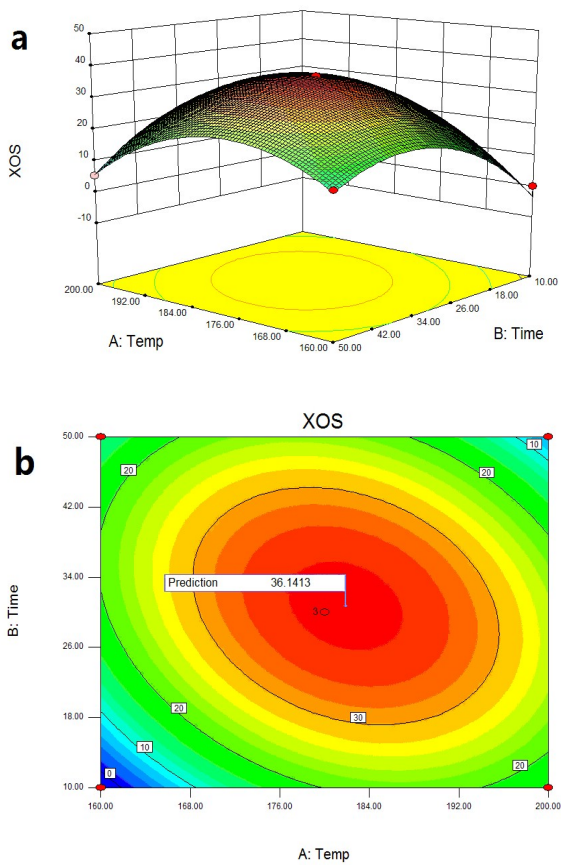


Fig. 2.

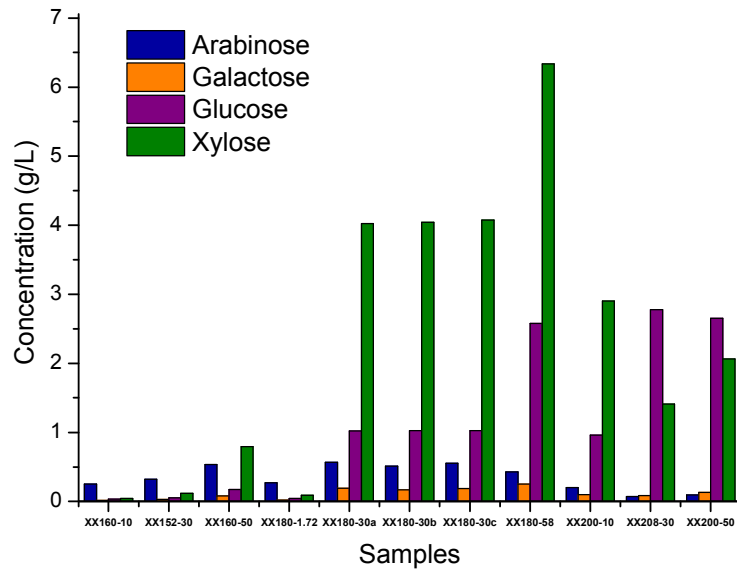


Fig. 3.

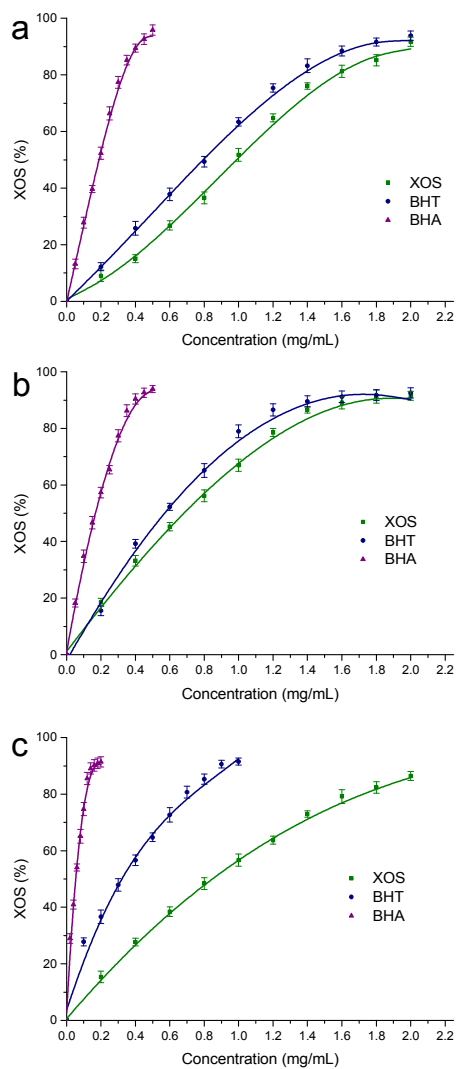
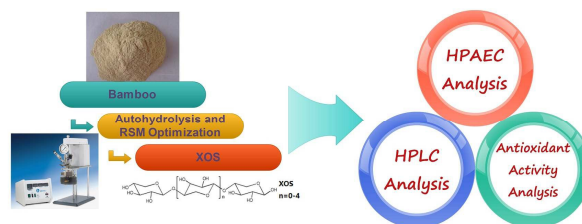


Fig. 4.

Table of Contents



Title: Optimization of bamboo autohydrolysis for the production of xylo-oligosaccharides using response surface methodology

Author(s): Xiao Xiao, Chen-Zhou Wang, Jing Bian* and Run-Cang Sun*

Synopsis: Bamboo was employed to generate xylo-oligosaccharides by using autohydrolysis, and the process was optimized via response surface methodology to achieve the highest yield.